

# A pair potential that reproduces the shape of isochrones in molecular liquids

Arno A. Veldhorst,<sup>\*</sup> Thomas B. Schröder,<sup>†</sup> and Jeppe C. Dyre<sup>‡</sup>

*“Glass and Time”, IMFUFA, Dept. of Sciences,  
Roskilde University, P.O. Box 260, DK-4000 Roskilde, Denmark*

(Dated: April 21, 2016)

Many liquids have curves (isomorphs) in their phase diagram along which structure, dynamics and some thermodynamic quantities are invariant in reduced units. A substantial part of their phase diagram is thus effectively one dimensional. The shape of these isomorphs is described by a material-dependent function of density  $h(\rho)$ , which for many liquids is well approximated by a power law  $\rho^\gamma$ . When density changes are large, however, this often fails; simulations of typical models such as the Lennard-Jones system show that  $\gamma(\rho) \equiv d \ln h(\rho) / d \ln \rho$  is a decreasing function of the density, while experimental results on organic liquids show the opposite. This paper presents results from computer simulations using a new pair potential that diverges at a non-zero distance and has  $\gamma(\rho)$  increasing with density. Our results indicate that the finite size of molecules should be taken into account when modeling liquids over a large density range.

It is still an open question what controls the dynamics of viscous, glass-forming liquids [1–6]. Although the dynamics in general depends on both temperature  $T$  and density  $\rho$ , the dynamics of many organic supercooled liquids can be collapsed onto a single curve when plotted against a combined, material-specific variable  $h(\rho)/T$  [7–9]. It was found in many experiments that the scaling function  $h(\rho)$  is generally well approximated by a power law as  $h(\rho) = \rho^\gamma$ , with  $\gamma$  being the material-specific density-scaling exponent [10, 11]; we refer to this as *power-law density scaling*. Another important development was the discovery that the dynamics of liquids are a function of the excess entropy [12, 13].

The isomorph theory [14] explains why both density scaling and excess-entropy scaling work for some liquids. Liquids that obey the isomorph theory have curves in their phase diagram, so-called isomorphs, along which not only the dynamics, but also the structure, excess entropy and other thermodynamic quantities are invariant. The development of the isomorph theory was initiated by the observation that in computer simulations some liquids have correlated fluctuations in their energy and pressure. More specifically, if the energy  $E$  and pressure  $p$  are split in a kinetic part and a configurational part that only depends on the particle positions  $\mathbf{R} \equiv \mathbf{r}_1, \dots, \mathbf{r}_N$ , as follows

$$\begin{aligned} E &= K + U(\mathbf{R}), \\ pV &= Nk_B T + W(\mathbf{R}), \end{aligned} \quad (1)$$

the correlations are found between the thermal equilibrium fluctuations of the potential energy  $U$  and the virial  $W$  in the  $NVT$  ensemble [15], although the correlations have also been found at high pressures in the  $NpT$  en-

semble [16]. Indeed, the standard correlation coefficient

$$R = \frac{\langle \Delta W \Delta U \rangle}{\sqrt{\langle (\Delta W)^2 \rangle \langle (\Delta U)^2 \rangle}} \quad (2)$$

indicates whether a liquid obeys the isomorph theory: this is the case whenever  $R > 0.9$  (although this value is of course somewhat arbitrary). The standard linear regression “slope” of the fluctuations

$$\gamma \equiv \frac{\langle \Delta W \Delta U \rangle}{\langle (\Delta U)^2 \rangle} \quad (3)$$

is the density-scaling exponent [14], and the theory thus provides a convenient way to determine the density-scaling exponent in computer simulations.

Another empirical observation that can be explained by the theory is that many liquids have been shown to obey isochronal superposition, meaning that a liquid’s relaxation spectra have identical shape if the average relaxation time is the same [17–19]. Also certain phenomenological melting rules can be explained by the isomorph theory [20–22]. The Lindemann melting criterion for instance states that crystals melt when their vibrational displacement reaches a certain value in reduced units. This follows from the theory since the melting line is predicted to be an isomorph to a good approximation [14], and indeed many other properties have also been found to be isomorphic on the melting line [23–25].

Many model systems studied so far have been shown to obey the isomorph theory, including atomic liquids with a range of different pair potentials [26–29], crystals [30], as well as rigid [31] and flexible molecular liquids [32]. Experimental evidence for the isomorph theory proved harder to get, but has been provided as well [33–35]. For a detailed description of the isomorph theory focusing on its validation in simulations and experiments, the reader is referred to a recent Feature article [36].

The isomorph theory has been tested most thoroughly in computer simulations. In simulations it is possible to investigate much larger ranges of density than in experiments. Interestingly, it was discovered that when large

<sup>\*</sup> a.a.veldhorst@gmail.com; Current Address: Laboratório de Espectroscopia Molecular, Instituto de Química, Universidade de São Paulo, CP 26077, CEP 05513-970 São Paulo, SP, Brazil

<sup>†</sup> tbs@ruc.dk

<sup>‡</sup> dyre@ruc.dk

differences in density were considered, power-law density scaling does not hold [37]. Instead, the scaling function  $h(\rho)$ , which describes the isomorphs via the equation  $h(\rho)/T = \text{Const.}$ , is a more general function of density. Inverse power-law potentials with  $v(r) \propto r^n$  obey power-law density scaling exactly (with  $\gamma = n/3$ ) and have perfectly correlated fluctuations in  $U$  and  $W$  ( $R = 1$ ). For other model liquids,  $h(\rho)$  is not known analytically although it can be determined from a single simulation if the pair potential is a sum of inverse power laws, as is the case for the well-known Lennard-Jones pair potential [38]. In that case each power-law term  $n$  in the potential leads to a term in  $h(\rho)$ , with the relative contribution of that term to the excess heat capacity  $C_V^{ex} = \sum_n C_{V,n}^{ex}$  as the prefactor [37]

$$h(\rho) = \sum_n \frac{C_{V,n}^{ex}}{C_V^{ex}} \rho^{n/3}. \quad (4)$$

The relative contributions to  $C_V^{ex}$  of each term in the potential can easily be determined from a single simulation.

Recently, new experimental results on the organic liquids dibutylphthalate (DBP) and decahydroisoquinoline (DHIQ) have shown that  $h(\rho)$  is indeed not well described by a power law when density changes are large enough (up to 20%) [37]. Instead the (logarithmic) slope of  $h(\rho)$

$$\gamma(\rho) = \frac{d \ln h(\rho)}{d \ln \rho}, \quad (5)$$

which gives the “local” density-scaling exponent, is an increasing function of density. This is in contrast to results from computer simulations, which usually show that  $\gamma$  decreases with density for atomic liquids with different pair potentials [26–28], as well as for molecular systems [31, 32, 39]. The fact that the Lennard-Jones potential has a decreasing  $\gamma(\rho)$  can be understood by considering that at high densities, particles are close to each other and only feel the repulsive  $r^{-12}$  term. For high densities,  $\gamma$  should thus approach  $12/3 = 4$ . At normal densities (around zero pressure), the attractive  $r^{-6}$  term plays an important role, however, and because it is subtracted it makes the Lennard-Jones potential steeper than the  $r^{-12}$  inverse power law. At low pressure, the Lennard-Jones potential therefore has a higher scaling exponent than expected from its  $r^{-12}$  term, and one finds here  $\gamma \approx 6$  [26].

A potential that has increasing  $\gamma(\rho)$  would have to contain increasingly steep power laws. This led us to suggest a sum of infinitely many power laws

$$\int_p^\infty r^{-n} dn \quad (6)$$

as a candidate. For it to be a more realistic model of a molecular liquid, we also included an attraction as

$$A \int_p^\infty r^{-n} dn - B \int_q^\infty r^{-n} dn = A \frac{r^{-p}}{\ln(r)} - B \frac{r^{-q}}{\ln(r)}, \quad (7)$$

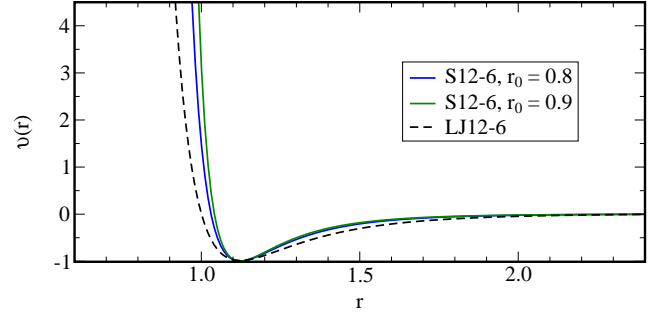


FIG. 1. The S12-6 pair potential as described in Eq. (8) plotted for two values of  $r_0$ , compared to the standard 12-6 Lennard-Jones (LJ) pair potential. The minimum was kept at  $r_m = 2^{1/6}$  to make the two potentials comparable to the LJ potential, which is shown by the dashed line.

with  $p > q$ . This potential diverges at  $r_0 = 1$ , but to easily set the potential minimum  $r_m$ , the divergence diameter  $r_0$ , and the potential depth  $\varepsilon$  we parameterize the potential as

$$v(r) = \varepsilon \frac{A (r/r_m)^{-p} - B (r/r_m)^{-q}}{\ln(r/r_0)}, \quad (8)$$

where

$$A = \frac{q \ln(r_m/r_0) + 1}{p - q},$$

$$B = \frac{p \ln(r_m/r_0) + 1}{p - q}.$$

In this study, we choose the exponents  $p = 12$  and  $q = 6$ , like the standard Lennard-Jones potential, and we name it the S12-6 potential.

## I. SIMULATION PROCEDURE

The S12-6 pair potential is plotted in Fig. 1. In order to get densities comparable to the Lennard-Jones liquid, the position of the potential minimum was chosen to be the same ( $\varepsilon = 1$  and  $r_m = 2^{1/6}$ ). This means that we use the Lennard-Jones parameter  $\sigma = 2^{-1/6} r_m$  as the unit of length. Two values of the hard-core radius were simulated ( $r_0 = 0.8$  and  $r_0 = 0.9$ ). The ratio  $r_m/r_0$  can be considered a measure for the steepness of the repulsion; it is respectively 1.247 and 1.403 in these cases. The potential was cut and shifted at 2.5.

A cubic box with periodic boundary conditions and 1000 particles was simulated in the  $NVT$  ensemble with a Nosé-Hoover thermostat. The integration time step was 0.001 for most state points, but it was decreased at high temperatures and densities in order to prevent unphysically large particle displacements. At each state point an initial configuration was first randomized by simulating the desired temperature for  $2^{22}$  steps at four times,

followed by an equilibration run and a production run of  $2^{24}$  time steps at the desired temperature.

The simulations were performed using the RUMD code [40]. This code is optimized for GPU computing and designed to make implementation of new interparticle potentials straightforward [41].

## II. RESULTS AND DISCUSSION

A configuration  $\mathbf{R}$  is expressed in reduced (dimensionless) units by scaling with the density as  $\rho^{1/3}\mathbf{R}$ . Two state points  $(\rho_1, T_1)$  and  $(\rho_2, T_2)$  are defined to be isomorphic if configurations  $\mathbf{R}_1$  and  $\mathbf{R}_2$  of those state points with same reduced coordinates,

$$\rho_1^{1/3}\mathbf{R}_1 = \rho_2^{1/3}\mathbf{R}_2, \quad (9)$$

also have proportional Boltzmann statistical weights [14]:

$$\exp\left(-\frac{U(\mathbf{R}_1)}{k_B T_1}\right) = C_{1,2} \exp\left(-\frac{U(\mathbf{R}_2)}{k_B T_2}\right). \quad (10)$$

In practice, this proportionality should hold to a good approximation for most physically relevant configurations of the two state points with the same constant  $C_{1,2}$  (which only depends on the pair of state point). Recently, a more general definition of the isomorph theory has been discovered [42], but we use here the “older” definition (Eq. (10)) as it is more convenient for generating isomorphic state points in simulations.

The isomorph definition can be used to obtain a set of isomorphic state points from a simulation at an initial state point, by rewriting Eq. (10) as

$$U(\mathbf{R}_2) = \frac{T_2}{T_1}U(\mathbf{R}_1) + k_B T_2 \ln(C_{1,2}). \quad (11)$$

Doing a standard equilibrium  $NVT$  simulation at some initial state point 1, one calculates for each configuration first  $U(\mathbf{R}_1)$  and subsequently  $U(\mathbf{R}_2)$  by scaling to a new density  $\rho_2$  using Eq. (9). According to Eq. (11), the energies of the scaled configurations should be linear proportional to the energies of the initial configurations with proportionality constant  $T_2/T_1$ . In this way the temperature  $T_2$  for which the state point at density  $\rho_2$  is isomorphic to state point 1 is given by the slope in an  $U(\mathbf{R}_1)$ ,  $U(\mathbf{R}_2)$  plot.

The intermediate scattering function  $F_S(q, t)$  and the radial distribution function  $g(r)$  along two isomorphs are plotted in Fig. 2 in reduced units defined,  $\tilde{t} \equiv t\rho^{1/3}\sqrt{k_B T}$  and  $\tilde{r} \equiv r\rho^{1/3}$ . For  $\rho = 0.9$  and  $r_0 = 0.9$  the effect on the dynamics of increasing the temperature by a factor of two while keeping density constant is also shown (dashed green line). The isochoral temperature change has a significant effect on the dynamics, while there is no significant change in  $F_S$  along the isomorph, where temperature changes by a factor of 22. These data indicate that we have indeed obtained two sets of isomorphic

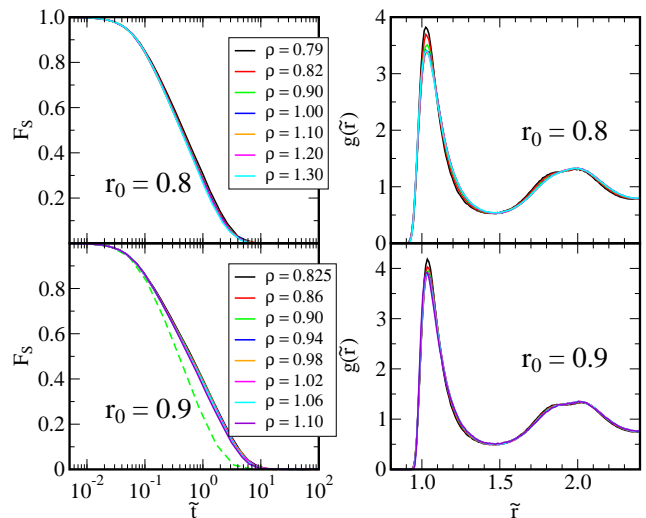


FIG. 2. The incoherent intermediate scattering function (left) and the radial distribution function (right) in reduced units, for the potentials with hard core diameter  $r_0 = 0.8$  (top) and  $r_0 = 0.9$  (bottom). For both isomorphs, the dynamics and structure are invariant to a high degree. All intermediate scattering functions have been calculated with the same reduced wave vector ( $\tilde{q} = 7.11$ ). The dashed green line shows the effect of an isochoral ( $\rho = 0.9$ ) temperature change for comparison.

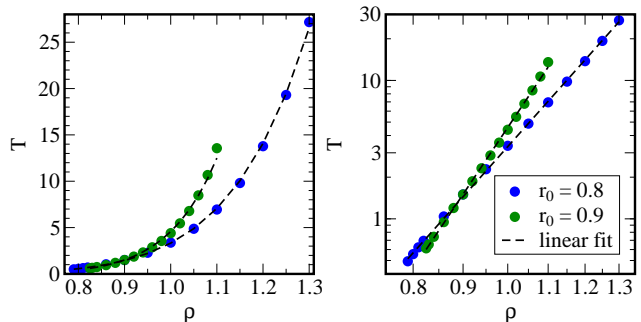


FIG. 3. The shape of the isomorphs in the  $\rho, T$  phase diagram on a linear scale (left) and a log-log scale (right). The shape of the isomorph is dependent on the hard-core diameter  $r_0$ . On the log-log scale, the isomorphs appear to be fitted well by a straight lines (dashed lines).

state points since both the dynamics and the structure are invariant in reduced units to a good approximation along the isomorph. There is a small change in the first peak of  $g(r)$ , though, which is expected since at high density the particles are close and feel a steeper part of the potential. This leads to a steeper and therefore higher peak in  $g(r)$  [29].

The shape of the isomorphs in the  $\rho, T$  plane is shown in Fig. 3 in a linear (a) and a double logarithmic scale (b). There is a clear effect of the particle diameter  $r_0$ . For  $\gamma$  to be constant along the isomorph ( $h(\rho) \propto \rho^\gamma$ ), the isomorph should be a straight line in the log-log plot. There is barely any deviation from linear fits (dashed lines) in

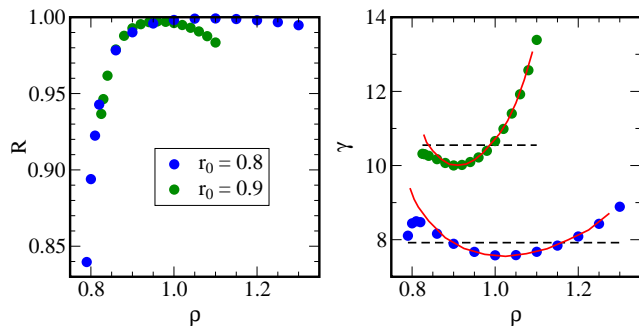


FIG. 4. The correlation coefficient  $R$  (left) and  $\gamma$  (right) as a function of density, calculated from the fluctuations (Eq. (2) and Eq. (2), green and blue dots). The red lines are finite difference estimates (see Eq. (5)) of the data in Fig. 3. For both hard core diameters  $r_0$  the  $U, W$  correlations are strong, and  $\gamma$  increases at high densities.

Fig. 3(a), indicating that a power law is a good approximation. From the fits we find approximate “constant  $\gamma$ ” values of 7.92 and 10.55 respectively for  $r_0 = 0.8$  and  $r_0 = 0.9$ .

As mentioned, liquids that obey the isomorph theory have strong correlations in the instantaneous values of the potential energy  $U$  and the virial  $W$ . We investigate these correlations in Fig. 4 plotting the correlation coefficient  $R$  and the “slope”  $\gamma$  from a linear regression of  $U, W$  data (Eq. (3)). The liquids have strong correlations at all state points; only close to the gas-liquid coexistence region, where the pressure becomes negative, is there a significant decrease in  $R$ . This is commonly found in many liquids when the pressure approaches zero [26].

Although the isomorphs are fitted well by a straight line in Fig. 3, the change in  $\gamma$  is considerable when calculated from the logarithmic slope of  $\rho, T$  data (red line). For both particle sizes we see an initial decrease of  $\gamma$  at low densities, similar to what is seen for liquids consisting of point particles like the Lennard-Jones liquid [26]. However, unlike such standard systems,  $\gamma$  increases again at higher densities. This density increase is stronger when

the hard-core radius is closer to the potential minimum. This result gives a possible explanation of why molecular liquids have been found to have an increasing  $\gamma(\rho)$  [37]. The two organic liquids DBP and DHIQ for which this has been found have atomic weights of 278 g/mol and 138 g/mol, respectively. These molecules are clearly not point particles, and based on the above we suggest that the increasing  $\gamma(\rho)$  is caused simply by the finite volume of these molecules. Our results show the importance of the potential shape when large density changes are involved, especially when molecular liquids are simulated using coarse-grained models, as in this case it is common to use Lennard-Jones potentials that diverge at zero distance [43–45].

We note that so far only one other pair potential gives an increasing  $\gamma(\rho)$ , which is the Girifalco potential [46]. This potential was developed to model  $C_{60}$  (Buckminsterfullerene), and the size of the  $C_{60}$  molecule led to a functional form that also diverges at non-zero interparticle distance.

To conclude, our results for the S12-6 pair potential shed light on the discrepancy between experiments and simulation concerning the behavior of the density-scaling exponent  $\gamma(\rho)$ . We suggest that the decreasing  $\gamma(\rho)$  seen in most simulations is a result of the potential used (often a Lennard-Jones type potential). On the other hand, the increasing value of  $\gamma(\rho)$  seen in experiments with molecular liquids seems to be an effect of the finite size of the molecules involved which is mimicked by the new S12-6 pair potential defined in Eq. (8). Our results indicate that the size of molecules should be considered when choosing a pair potential to model a liquid over a large range of densities.

## ACKNOWLEDGMENTS

This work was sponsored by the Danish National Research Foundation via Grant No. DNRF61.

- 
- [1] P. G. Debenedetti and F. H. Stillinger, *Nature* **410**, 259 (2001).
  - [2] J. C. Dyre, *Rev. Mod. Phys.* **78**, 953 (2006).
  - [3] V. Lubchenko and P. G. Wolynes, *Annu. Rev. Phys. Chem.* **58**, 235 (2007).
  - [4] S. A. Kivelson and G. Tarjus, *Nat. Mater.* **7**, 831 (2008).
  - [5] A. Cavagna, *Phys. Rep.* **476**, 51 (2009).
  - [6] M. D. Ediger and P. Harrowell, *J. Chem. Phys.* **137**, 080901 (2012).
  - [7] A. Tölle, H. Schober, J. Wuttke, O. G. Randl, and F. Fajara, *Phys. Rev. Lett.* **80**, 2734 (1998).
  - [8] C. Alba-Simionesco, D. Kivelson, and G. Tarjus, *J. Chem. Phys.* **116**, 5033 (2002).
  - [9] G. Tarjus, D. Kivelson, S. Mossa, and C. Alba-Simionesco, *J. Chem. Phys.* **120**, 6135 (2004).
  - [10] C. M. Roland, S. Hensel-Bielowka, M. Paluch, and R. Casalini, *Reports Prog. Phys.* **68**, 1405 (2005).
  - [11] C. M. Roland, *Macromolecules* **43**, 7875 (2010).
  - [12] Y. Rosenfeld, *Phys. Rev. A* **15**, 2545 (1977).
  - [13] M. Dzugutov, *A universal scaling law for atomic diffusion in condensed matter* (1996).
  - [14] N. Gnan, T. B. Schrøder, U. R. Pedersen, N. P. Bailey, and J. C. Dyre, *J. Chem. Phys.* **131**, 234504 (2009).
  - [15] U. R. Pedersen, N. P. Bailey, T. B. Schrøder, and J. C. Dyre, *Phys. Rev. Lett.* **100**, 015701 (2008).
  - [16] D. Coslovich and C. M. Roland, *J. Chem. Phys.* **130**, 014508 (2009).
  - [17] A. Tölle, *Reports Prog. Phys.* **64**, 1473 (2001).
  - [18] C. M. Roland, R. Casalini, and M. Paluch, *Chem. Phys. Lett.* **367**, 259 (2003).

- [19] K. L. Ngai, R. Casalini, S. Capaccioli, M. Paluch, and C. M. Roland, *J. Phys. Chem. B* **109**, 17356 (2005).
- [20] J. J. Gilvarry, *Phys. Rev.* **102**, 308 (1956).
- [21] M. Ross, *Phys. Rev.* **184**, 233 (1969).
- [22] F. Saija, S. Prestipino, and P. V. Giaquinta, *J. Chem. Phys.* **124**, 244504 (2006).
- [23] D. M. Heyes, D. Dini, and A. C. Brańka, *Phys. Status Solidi B* (2015).
- [24] D. M. Heyes and A. C. Brańka, *J. Chem. Phys.* **143**, 234504 (2015).
- [25] L. Costigliola, T. B. Schröder, and J. C. Dyre (2016), URL <http://arxiv.org/abs/1602.03355>.
- [26] N. P. Bailey, U. R. Pedersen, N. Gnan, T. B. Schröder, and J. C. Dyre, *J. Chem. Phys.* **129**, 184507 (2008).
- [27] A. A. Veldhorst, L. Böhling, J. C. Dyre, and T. B. Schröder, *Eur. Phys. J. B* **85**, 21 (2012).
- [28] A. K. Bacher, T. B. Schröder, and J. C. Dyre, *Nat. Commun.* **5**, 5424 (2014).
- [29] A. A. Veldhorst, T. B. Schröder, and J. C. Dyre, *Phys. Plasmas* **22**, 073705 (2015).
- [30] D. E. Albrechtsen, A. E. Olsen, U. R. Pedersen, T. B. Schröder, and J. C. Dyre, *Phys. Rev. B* **90**, 094106 (2014).
- [31] T. S. Ingebrigtsen, T. B. Schröder, and J. C. Dyre, *J. Phys. Chem. B* **116**, 1018 (2012).
- [32] A. A. Veldhorst, J. C. Dyre, and T. B. Schröder, *J. Chem. Phys.* **141**, 054904 (2014).
- [33] N. P. Bailey, U. R. Pedersen, N. Gnan, T. B. Schröder, and J. C. Dyre, *J. Chem. Phys.* **129**, 184508 (2008).
- [34] D. Gundermann, U. R. Pedersen, T. Hecksher, N. P. Bailey, B. Jakobsen, T. Christensen, N. Boye Olsen, T. B. Schröder, D. Fragiadakis, R. Casalini, et al., *Nat. Phys.* **7**, 816 (2011).
- [35] W. Xiao, J. Tofteskov, T. V. Christensen, J. C. Dyre, and K. Niss, *J. Non. Cryst. Solids* **407**, 190 (2015).
- [36] J. C. Dyre, *J. Phys. Chem. B* **118**, 10007 (2014).
- [37] L. Böhling, T. S. Ingebrigtsen, A. Grzybowski, M. Paluch, J. C. Dyre, and T. B. Schröder, *New J. Phys.* **14**, 113035 (2012).
- [38] T. S. Ingebrigtsen, L. Böhling, T. B. Schröder, and J. C. Dyre, *J. Chem. Phys.* **136**, 061102 (2012).
- [39] T. B. Schröder, U. R. Pedersen, N. P. Bailey, S. Toxvaerd, and J. C. Dyre, *Phys. Rev. E* **80**, 041502 (2009).
- [40] *Roskilde University Molecular Dynamics*, URL <http://rumd.org>.
- [41] N. P. Bailey, T. S. Ingebrigtsen, J. S. Hansen, A. A. Veldhorst, L. Böhling, C. A. Lemarchand, A. E. Olsen, A. K. Bacher, H. Larsen, J. C. Dyre, et al. (2015), URL <http://arxiv.org/abs/1505.05094>.
- [42] T. B. Schröder and J. C. Dyre, *J. Chem. Phys.* **141**, 204502 (2014).
- [43] W. Shinoda, R. DeVane, and M. L. Klein, *Mol. Simul.* **33**, 27 (2007).
- [44] S. Riniker, J. R. Allison, and W. F. van Gunsteren, *Phys. Chem. Chem. Phys.* **14**, 12423 (2012).
- [45] S. J. Marrink and D. P. Tieleman, *Chem. Soc. Rev.* **42**, 6801 (2013).
- [46] N. P. Bailey, L. Böhling, A. A. Veldhorst, T. B. Schröder, and J. C. Dyre, *J. Chem. Phys.* **139**, 184506 (2013).